Dalton Transactions

Cite this: *Dalton Trans.*, 2011, **40**, 92

www.rsc.org/dalton

PAPER

Tuning the conversion of cyclohexane into cyclohexanol/one by molecular dioxygen, protons and reducing agents at a single non-porphyrinic iron centre and chemical versatility of the tris(2-pyridylmethyl)amine TPAFe^{II}Cl$_2$ complex in mild oxidation chemistry†

Hassen Jaafar,[a] Bertrand Vileno,[b] Aurore Thibon[a] and Dominique Mandon*[a]

Received 30th June 2010, Accepted 28th September 2010
DOI: 10.1039/c0dt00756k

We report that the oxygen sensitivity of some Fe(II) complexes with tripodal ligands can be used, with benefit, in the oxidation of cyclohexane under mild conditions. Depending on the solvent, two very different reaction pathways are involved, which share the coordination of O_2 to the metal as the common initial step. We have synthesized a series of α-chlorinated tripods in the tris(2-pyridylmethyl)amine series Cl$_n$TPA (n = 1–3) and fully characterized the corresponding FeX_2 complexes (X = Cl, CF_3SO_3). The single-crystal X-ray structure analyses of the $FeCl_2$ complexes are reported. In CH_3CN, the $FeCl_2$ complexes react smoothly with O_2, whereas the $Fe(CF_3SO_3)_2$ complexes are non-sensitive. In CH_3CN, the reaction of the oxygen-sensitive Cl$_n$TPAFeCl$_2$ (n = 0–3) with O_2, acetic acid and zinc amalgam, in the presence of cyclohexane, affords a mixture of cyclohexanol/one in an ≈ ol/one ratio of 3.1 and a selectivity of the C3°/C2° in the adamantane conversion that is consistent with a metal-oxo based oxidation. Limited efficiency (≈ 2 TON) was observed for the parent TPAFeCl$_2$ complex and Cl$_1$TPAFeCl$_2$, whereas both other complexes turned out to be poorly active. The TPAFeCl$_2$ complex was used to address mechanistic questions: when the reaction was carried out in pyridine, the ol/one ratio shifted to 0.15 while efficiency was improved by 7-fold. In pyridine and in the presence of a spin trap (DMPO), the radical-based character of the reaction was definitely established, by contrast with acetonitrile, where no oxygenated radicals were detected. Thus, the reactivity differences arise from involvement of two distinct active species. The dichotomous radical/biomimetic pathway is discussed to interpret these results.

1. Introduction

Setting up mild conditions in oxidation processes involving molecular dioxygen remains, more than 25 years after the first report of the "Gif reaction", a real challenge in the current economical context.[1–3] In biological systems, dioxygen coordinates to mono- and dinuclear non-heme iron-containing centres present at active sites of proteins and is activated in such a way that major transformations can be realized.[4–7] Following extensive studies involving various metal centres,[8,9] the biomimetic activation of the C–H bond by iron complexes emerged as a very attractive approach.[9–11] The use of small coordination complexes is indeed rising as a promising approach: recent developments shed light on the ability of small iron complexes to perform site- and stereospecific oxidation of various substrates, ranging from simple alkanes to terpenoids.[12–15] In spite of the restricted exceptions involving dinuclear iron-containing complexes,[16,17] hydrogen peroxide is generally used as the oxidant. Molecular oxygen, which is involved in many biological processes, and is a universally available and safe resource, would be more convenient to use. However, its activation by cheap metal complexes is far from been scientifically solved. Thus, there is still a wide open investigation field in this area, from both academic and technological points of view.

In the course of our investigations with $FeCl_2$ complexes of tripodal ligands [the parent tris(2-pyridylmethyl)amine (TPA) ligand or some α-substituted tripods], we have already reported that the O_2 mediated conversion of $FeCl_2$ complexes into μ-oxo diferric stable complexes is a general reaction involving the coordination of dioxygen to the iron centre.[18,19]

[a]*Laboratoire de Chimie Biomimétique des Métaux de Transition, Institut de Chimie, UMR CNRS no. 7177, Université de Strasbourg, 4 rue Blaise Pascal, B.P. 1032, F-67070 Strasbourg cedex, France. E-mail: mandon@chimie.u-strasbg.fr; Fax: 33-(0)368-851-438; Tel: 33-(0)368-851-537*

[b]*Laboratoire des Propriétés Optiques & Magnétiques des Architectures Moléculaires, Institut de Chimie, UMR CNRS n° 7177, Université de Strasbourg, 1 rue Blaise Pascal, B.P. 296/R8, F-67070, Strasbourg cedex, France*

† Electronic supplementary information (ESI) available: Spectroscopic data of all new compounds described in this study. Oxygenation curves of compound Cl$_1$TPAFeCl$_2$ and kinetic parameters. CCDC reference numbers 751029–751031. For ESI and crystallographic data in CIF or other electronic format see DOI: 10.1039/c0dt00756k

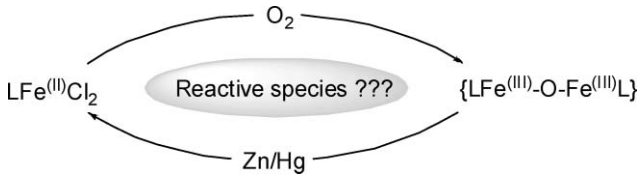

We demonstrated that molecular oxygen does coordinate to the metal centre by a mechanism involving dissociation of the Fe–Cl bond.[19] Additionally, with ligands substituted by non-innocent functional groups, in aprotic medium and in the absence of an exogenous substrate, intramolecular reactions mimicking the transformations encountered in biological systems (cleavage of esters,[19] oxidative dehydrogenation,[20] O-demethylation[21]) were found to take place in the vicinity of the metal centre.

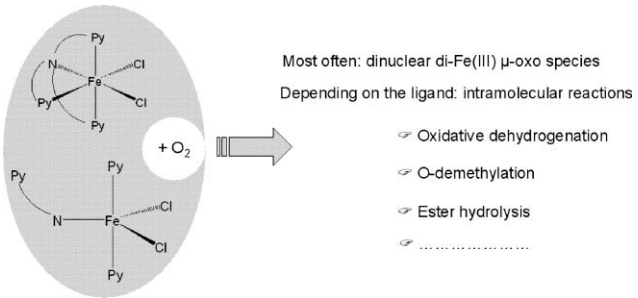

The process involved in these reactions requires activation of dioxygen by the iron centre, leading to generation of an active species. In our previously published articles reporting intramolecular reactivities, we tended to favour a superoxide-based mechanism resulting from inner sphere reduction of O_2 by the metal.[19,21] We could not however rule out a metal-oxo based pathway, in which the active species would be formed by homolytic cleavage of the O–O bond in a putative transient dinuclear species. If this were the case, an interesting reactivity towards exogenous substrates might be observed. In any event, it was tempting to address the question of whether or not any active species could perform C–H activation on an added substrate.

The question of sensitivity of the complexes towards dioxygen is a key point. In precedent studies, $FeCl_2$ complexes with α-fluorinated tris(2-pyridylmethyl)amine tripods were found to react smoothly with O_2.[18,22] We thought that increasing the steric hindrance around the metal centre might increase the lifetime of any potentially active species, allowing further chemistry to be done and decided to prepare the series of α-chlorinated ligands Cl_nTPA (n = 1, 2, 3). Herein we describe at first the structures of the corresponding $FeCl_2$ complexes and the preparation and spectroscopic characterization of the $Fe(OTf)_2$ analogues.

We then report that some of the oxygen-sensitive $FeCl_2$ complexes can, in acetonitrile, promote the conversion of cyclohexane into cylohexanol/one in mild conditions, yet with limited efficiency, using O_2, a reducing agent and a source of protons. Using $TPAFeCl_2$ as a comparison tool, we finally demonstrate the versatility of our system, the reaction profile being highly solvent-dependent. Whereas a classical "biomimetic" reactivity is observed in acetonitrile, pyridine promotes an oxygen-radical-based pathway, leading to the formation of ketone as the main product. On the basis of these results, and considering our previously reported work, a general reaction scheme is proposed, involving a first common step during which O_2 coordinates to the metal centre, followed by two different reaction pathways ("biomimetic" *vs.* "Gif"), depending on the presence (or not) of pyridine.

In a context where more and more studies describe the spectroscopic generation of potentially reactive intermediates from O_2 and protons,[23,24] our work represents one of the very few functional examples of biomimetic C–H hydroxylation of an inert substrate, by well-defined mononuclear non-porphyrinic iron complexes in mild conditions. In addition, we provide a positive approach to the long-time controversial question regarding the activation of O_2 by the $Fe^{(II)}$/AcOH/Zn system.[2]

2. Results

Synthesis

New α-chlorosubstituted derivatives $Cl_{1-3}TPA$ were synthesized following the classical pathway from 2-chloro-6-bromomethyl pyridine and corresponding amines.[18] Synthetic details and characterization can be found in the experimental section and as ESI.† These ligands were further complexed to $FeCl_2$ and $Fe(OTf)_2$ according to well-known procedures[18,25,26]

Coordination chemistry

The $FeCl_2$ complexes were obtained as yellow solid, thermally stable, yet oxygen-sensitive compounds. They were characterized by single-crystal X-ray diffraction and their molecular structure is displayed in Fig. 1. Whereas $Cl_1TPAFeCl_2$ and $Cl_3TPAFeCl_2$ display classical distorted octahedral and trigonal bipyramidal geometries, respectively, the iron centre in $Cl_2TPAFeCl_2$ is only moderately bound by the third pyridine, with Fe–N4 = 2.50 Å.

In an ideal octahedral symmetry, the plane defined by the tertiary amine and the two chloride atoms, $<N_{amine}Cl1Cl2$, should include, in the *trans* position to one the chloride ions (here Cl1), one pyridine nitrogen atom. This is, however, generally not the case; as already stated above, the classical picture is that of a distorted octahedral geometry, since the coordinated ligand defines a five-membered metallacycle with sharper angles, close to 76°.

$Cl_1TPAFeCl_2$ does not make exception to the rule, with the N3 atom standing 0.79 Å above the <N1Cl1Cl2 plane, the Fe atom being displaced by 0.19 Å. In $Cl_2TPAFeCl_2$, the displacement of the *trans* pyridine atom from the mean plane is only 0.18 Å, the Fe being displaced by 0.10 Å. This is certainly due to the elongation of the Fe–N4 bond, which by mechanical effect decreases the stress of the ligand, allowing a more classical arrangement around the metal centre in $Cl_2TPAFeCl_2$. Fig. 2 compares the situation in $Cl_1TPAFeCl_2$ and $Cl_2TPAFeCl_2$. Thus, in the solid state, the structure of $Cl_2TPAFeCl_2$ can be considered as being intermediate between that of $Cl_1TPAFeCl_2$ and $Cl_3TPAFeCl_2$.

In solution, the UV-vis spectrum of $Cl_1TPAFeCl_2$ displays an Fe → Py MLCT absorption at λ = 392 nm, with the molecular extinction coefficient ($\varepsilon = 1.2 \cdot 10^3$ mmol^{-1} cm^2) supporting tetradentate coordination of the tripod. Also, the presence of relatively sharp signals in the ^{1}H NMR spectra for this paramagnetic species confirms that the geometry as observed in the solid state is retained in solution.[25] By contrast, the spectroscopic data of solutions of $Cl_3TPAFeCl_2$ indicates hypodentate coordination of the tripod in

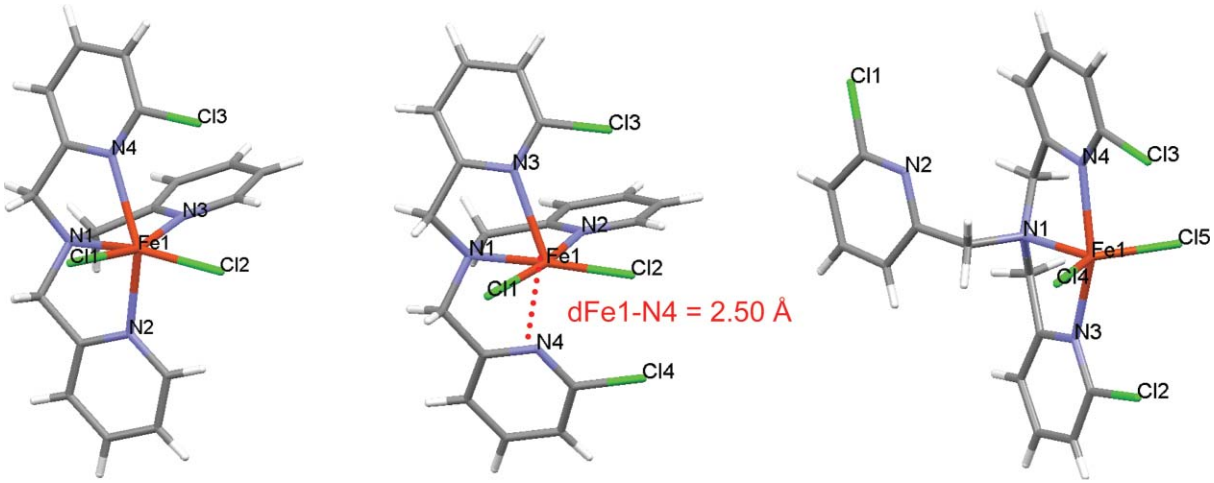

Fig. 1 Mercury drawing of $Cl_{1-3}TPAFeCl_2$ complexes. Left $Cl_1TPAFeCl_2$, Middle $Cl_2TPAFeCl_2$, Right $Cl_3TPAFeCl_2$. Details of the bond lengths are available from the cif files provided in the ESI.† All Fe–N bond lengths lie above 2.1 Å.

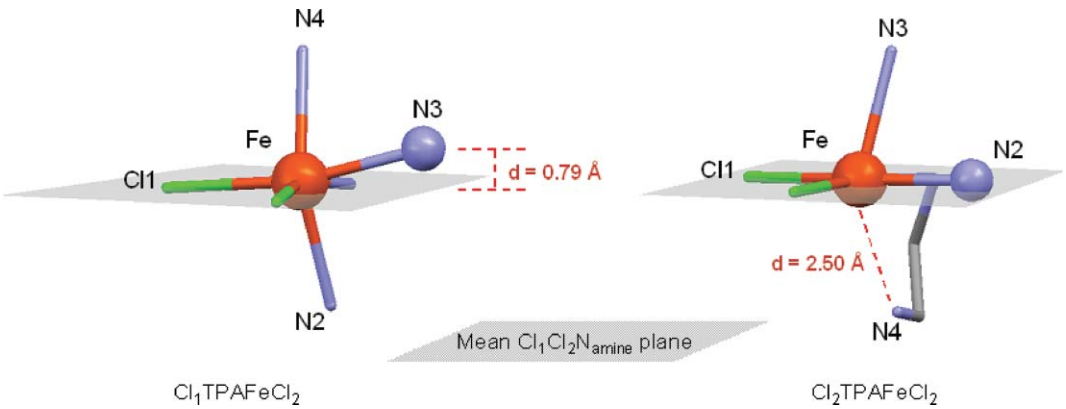

Fig. 2 Structural arrangement around the metal in complexes $Cl_1TPAFeCl_2$ and $Cl_2TPAFeCl_2$.

solution, as already observed with $F_3TPAFeCl_2$.[22,27] The MLCT absorption is almost nonexistent in UV-vis spectroscopy and extremely broad signals are detected in the ^1H NMR spectra. All data are given in the ESI.† Whereas in the solid state, the geometry around the metal in $Cl_2TPAFeCl_2$ can be considered as intermediate between that found in $Cl_1TPAFeCl_2$ and $Cl_3TPAFeCl_2$, solution studies unequivocally support hypodentate coordination of the tripod in this complex with a reduced intensity Fe → Py MLCT ($\varepsilon = 0.6{\cdot}10^3$ mmol^{-1} cm^2) absorption at $\lambda = 373$ nm and broad resonances in the ^1H NMR spectra, qualitatively similar to those already reported for $Br_2TPAFeCl_2$.[25]

The $Fe(OTf)_2$ complexes were obtained as solid materials, for which the colour was found to be highly dependent on the substitution of the ligand: a dark red solid was obtained for $TPAFe(OTf)_2$, the colour becoming beige-yellow in $Cl_1TPAFe(OTf)_2$, then grey in $Cl_2TPAFe(OTf)_2$ and finally light grey in $Cl_3TPAFe(OTf)_2$. The compounds turned out to be very hygroscopic,[28] yet they were stable to dioxygen, even in acetonitrile solutions. They were characterized by UV-vis, ^1H and ^{19}F NMR spectroscopies. All studies were performed in CH_3CN, the solvent in which further reactivity studies were carried out. It should be mentioned here that when dissolved in the coordinating solvents, the triflate anions are generally displaced by the solvent molecules, thus yielding dicationic species.[26,29]

In the UV-vis spectra in CH_3CN, the MLCT absorptions were found at $\lambda_1 = 354$ nm ($\varepsilon_1 = 1.3{\cdot}10^3$ mmol^{-1} cm^2), $\lambda_2 = 351$ nm ($\varepsilon_2 = 0.6{\cdot}10^3$ mmol^{-1} cm^2) and $\lambda_3 = 344$ nm ($\varepsilon_3 = 0.6{\cdot}10^3$ mmol^{-1} cm^2) for the $Cl_{1-3}TPAFe(OTf)_2$ complexes. In the ^1H NMR spectra, all of the complexes displayed relatively sharp and paramagnetically shifted signals over the +130 to +20 ppm range, in line with a high-spin state for the iron centre. With $Cl_1TPAFe(OTf)_2$, the ^{19}F NMR spectrum consisted of a sharp ($\Delta\nu_{1/2} = 35$ Hz) signal at $\delta = -72.1$ ppm. With $Cl_2TPAFe(OTf)_2$, the ^{19}F NMR spectrum exhibited a slightly broadened ($\Delta\nu_{1/2} = 90$ Hz) signal at $\delta = -74.1$ ppm, whereas more consequent, but still very limited, broadening ($\Delta\nu_{1/2} = 230$ Hz) was observed at $\delta = -74.2$ ppm in the spectrum of $Cl_3TPAFe(OTf)_2$. All these data, shown in the ESI,† support the presence of uncoordinated triflate ions in a CD_3CN solution, although minor broadening may arise from a limited dynamic exchange process in solution.[30]

Reactivity

Complexes–O_2. The $Cl_nTPAFeCl_2$ complexes react with O_2. For the six-coordinate-complexes, the sensitivity towards dioxygen can easily be quantified upon monitoring the UV-vis changes at a single wavelength, the changes leading to the formation of the final μ-oxo species. In general, two spectroscopic steps are

Table 1 Turnover numbers (product equiv./complex equiv.) observed in the H_2O_2 reaction. Cyclohexane : H_2O_2 : complex ratio 500 : 500 : 1. Addition time of H_2O_2: 4 h 30 min. All reactions were carried out in triplicate. When the reaction is carried out under O_2, the profile is not significantly modified

Complex	Cyclohexanol		Cyclohexanone		Total		A/K	
X	Cl	OTf	Cl	OTf	Cl	OTf	Cl	OTf
$TPAFeX_2$	18.9	25.0	9.8	7.4	28.7	32.4	1.9	3.4
$Cl_1TPAFeX_2$	18.1	15.9	7.8	3.9	25.9	19.8	2.3	3.8
$Cl_2TPAFeX_2$	9.3	9.8	5.7	4.6	15.0	14.4	1.6	2.1
$Cl_3TPAFeX_2$	1.2	2.7	1.1	1.2	2.3	3.9	1.1	2.2
FeX_2	3.5	13.5	2.2	4.3	5.7	17.8	1.6	3.1

observed.[18] With $Cl_1TPAFeCl_2$, we obtained $k_1 = 0.38$ and $k_2 = 0.052$ h^{-1}, *i.e.* in the same order of magnitude as the values found for the $TPAFeCl_2$ and $FTPAFeCl_2$ complexes.[18] The five-coordinate complexes generally exhibit transformation rates that are estimated to go *c.a.* 10–20 times faster.[18] This is the case with $Cl_2TPAFeCl_2$ and $Cl_3TPAFeCl_2$, for which total conversion was observed over 6 and 3 h, respectively.

Fe^{II} triflate complexes were also studied and exhibited no, or extremely limited, reactivity *vs.* O_2 when dissolved in CH_3CN. No tractable change could be observed in the UV-vis spectra, which remained unaffected even after several days of having dioxygen bubbled through the solution.

Complexes–H_2O_2–cylcohexane. The standard conditions for biomimetic oxidation reactions generally involve peroxides as the oxygen donors. We checked the activity of our compounds in the presence of hydrogen peroxide. Also, we compared the activities of the $Cl_{0-3}TPAFeCl_2$ and $Cl_{0-3}TPAFe(OTf)_2$ complexes, as weakly coordinating ligands are generally used as metal counter anions in biomimetic catalysis.[11]

As can be seen in Scheme 1 and Table 1, the conversion occurred when either type of complex was used as the catalyst. The triflate-coordinated compounds exhibited a slightly better reactivity than the chloride coordinated complexes. These results, which will be discussed later in this article, can be easily compared with those described in previous reports.[11,31,32,45,48]

Scheme 1 conversion of cyclohexane into cyclohexanol/one by the conventional H_2O_2 method.

Complexes–ZnHg–AcOH–O_2–cylclohexane. The $Cl_{0-3}TPAFeCl_2$ complexes being sensitive to dioxygen, their reactivity was tested in the presence of cyclohexane. The already known parent, the oxygen-sensitive $TPAFeCl_2$ complex, was also studied. 1.5 mg of each complex in 2 mL of dry and degassed acetonitrile was reacted with 0.35 mL of cyclohexane in the presence of dioxygen for the duration of 5 h. Three different conditions were investigated: (i) the medium "as is" was stirred during the reaction time, (ii) a drop of zinc amalgam was introduced before the addition of O_2 and (iii) 50 µL of acetic acid and a drop of zinc amalgam were introduced before the addition of O_2. At the end of the reaction time the medium was filtered and analyzed by gas chromatography.

Under the conditions of (i) and (ii), only trace amounts of the oxidation products could be detected, indicating that no tractable reaction occurred.

In the *simultaneous* presence of acetic acid *and* zinc amalgam, *i.e.* under the conditions of (iii), the conversion of cyclohexane into a mixture of cyclohexanol and cyclohexanone was observed, as displayed in Scheme 2.

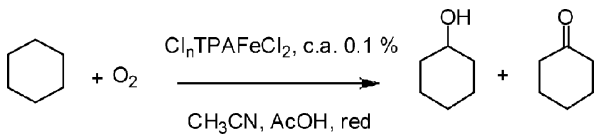

Scheme 2 conversion of cyclohexane into cyclohexanol/one in the presence of O_2, AcOH and $Cl_nTPAFeCl_2$ ($0<n<3$).

This conversion, however, is limited in yield: even if $TPAFeCl_2$ and $Cl_1TPAFeCl_2$ give more than a stoichiometric transformation based on the complex, this reaction can not be described as "catalytic" in the commonly accepted sense of the term. As indicated in Table 2, a significant amount of substrate is converted by the parent $TPAFeCl_2$ complex and $Cl_1TPAFeCl_2$, both compounds displaying a pseudo-octahedral geometry in solution, for which a smooth reactivity towards dioxygen was measured in the absence of the substrate. The five-coordinate complexes $Cl_2TPAFeCl_2$ and $Cl_3TPAFeCl_2$, although kinetically more reactive towards dioxygen, turned out to display a weaker reactivity, comparable to that of $FeCl_2$, when this salt was used alone in blank experiments. In the reaction conditions, the stability of these compounds turned out to be excellent and the observed lack of reactivity cannot be due to decomposition, indeed, µ-oxo diferric compounds are generally systematically recovered upon oxygenation of the medium (in the presence or absence of acetic acid). Finally, a blank experiment was carried out in the absence of the iron complex and no conversion was observed.

The mass balance, the mass spectroscopy analyses and the absence of other signals at long retention times in GC confirmed

Table 2 Turnover numbers (product equiv./complex equiv.) observed in the O_2–Zn–Hg reaction. Cyclohexane : AcOH : complex ratio 1100 : 300 : 1. A/K is the alcohol/ketone ratio. Reaction time: 5 h. All reactions were carried out at least five times

Complex	Cyclohexanol	Cyclohexanone	Total	A/K
$TPAFeCl_2$	1.6	0.5	2.1	3.2
$Cl_1TPAFeCl_2$	0.8	0.3	1.1	2.7
$Cl_2TPAFeCl_2$	0.4	0.2	0.5	2.0
$Cl_3TPAFeCl_2$	0.3	0.1	0.4	3.0
$FeCl_2$	0.2	0.1	0.3	2.0

Table 3 Turnover numbers (product equiv./complex equiv.) observed in the O_2–AcOH–red reaction of adamantane with $TPAFeCl_2$ in CH_3CN and pyridine. 3°/2° = 3 × (1-adamantanol)/(2-adamantanol + 2-adamantanone). The reactions were carried out in triplicate

	1-adamantanol	2-adamantanol	2-adamantanone	3°/2°
CH_3CN	2.5	0.7	0.6	5.8
Pyridine	2.6	0.7	3.5	1.8

that cyclohexanol and cyclohexanone were the only reaction products.

Focus on the $TPAFeCl_2$–ZnHg–AcOH–O_2 catalytic system. The parent $TPAFeCl_2$ being the most reactive complex, additional detailed studies were carried out with this compound. Cyclohexane was replaced by cyclohexanol as the substrate and the reaction was carried out in identical conditions. The GC analysis revealed that no trace of cyclohexanone could be detected. The composition of the medium remained unchanged.

Additionally, the C3°/C2° ($C_{Tertiary}/C_{Secondary}$) selectivity was tested in the oxidation of adamantane. The results are shown in Table 3. Although these are not as high as the reported values obtained from H_2O_2 as the oxygen donor and triflate or perchlorate salts with related ligands,[11,31] the 3°/2° ratio = 5.8 with the O_2–AcOH–ZnHg system significantly differs from that obtained when the HO• radical is used.[33–35]

With $TPAFeCl_2$ only, another set of experiments was defined, in conditions comparable to those involved in the Gif[IV] systems, *i.e.* with pyridine used as the reaction solvent. In pyridine d^5, the ^1H NMR spectrum of $TPAFeCl_2$ was not significantly different than in CH_3CN, confirming the high-spin state of the metal centre in this solvent (the ^1H-NMR and UV-vis data are given in the ESI†). The comparison between CH_3CN and pyridine as the solvent is spectacular in terms of the product distribution, as can be seen in Scheme 3.

Whereas a low efficiency was observed in CH_3CN (see above, and entry A in Table 4), the use of pyridine as the solvent allows a very significant increase in the conversion rate, switching the turnover from 2 to 15 (entry C in Table 4). Also, the production of ketone was clearly favoured in pyridine with a ketone/alcohol ratio of above 6 (A/K = 0.15).

Table 4 Turnover numbers (product equiv./complex equiv.) observed in the O_2–AcOH–red reaction with $TPAFeCl_2$ and $FeCl_2$, as a function of the reaction solvent (identical reaction conditions). Entry B: Cyclohexane : AcOH : pyridine : complex ratio 1100 : 300 : 300 : 1. All reactions were carried out at least five times

entry	Complex	C6-ol	C6-one	Total	A/K
A	$TPAFeCl_2$–H_3CN	1.6	0.5	2.1	3.2
B	$TPAFeCl_2$–CH_3CN + *PyHOAc*	1.4	1.6	3.1	0.9
C	$TPAFeCl_2$–pyridine	2.0	13.1	15.1	0.15
D	$FeCl_2$–CH_3CN	0.2	0.1	0.3	3.0
E	$FeCl_2$–pyridine	0.5	2.8	3.3	0.2

In acetonitrile, the presence of an equimolar mixture of pyridine and acetic acid in limited amounts resulted in a slight increase of the activity, with, however, a significant change in the selectivity.

To gain an insight into the reaction mechanisms, we carried out the oxygenations in acetonitrile and in pyridine in the presence of 5,5-dimethyl-1-pyrroline-*N*-oxide (DMPO), a spin trap commonly used in EPR to detect the presence of superoxide $O_2^{\bullet-}$ or OH• radicals,[36–38] as shown in Scheme 4.

DMPO was added to the substrate-containing solution and O_2 was subsequently added to this medium. The medium was stirred for 5 min and then a 50 μL aliquot of the solution was introduced into a glass capillary and immediately positioned in the EPR cavity. The measurements were performed at room temperature. The results are displayed in Scheme 4. No significant signal was detected, in any case, in the absence of oxygen. Unambiguously, no significant persistent radical species could be detected in the acetonitrile after the introduction of oxygen. By contrast, in pyridine an intense signal was detected, corresponding to the reactive oxygen species trapped by the DMPO, indicating direct evidence of the presence of the superoxide anion $O_2^{\bullet-}$, OH• radical and minor amounts of some thermal conversion products.[36–40]

A low temperature EPR search was performed over a broader field and no metal-related paramagnetic compounds, such as a ferric hydroperoxide species for instance, were detected. Whereas

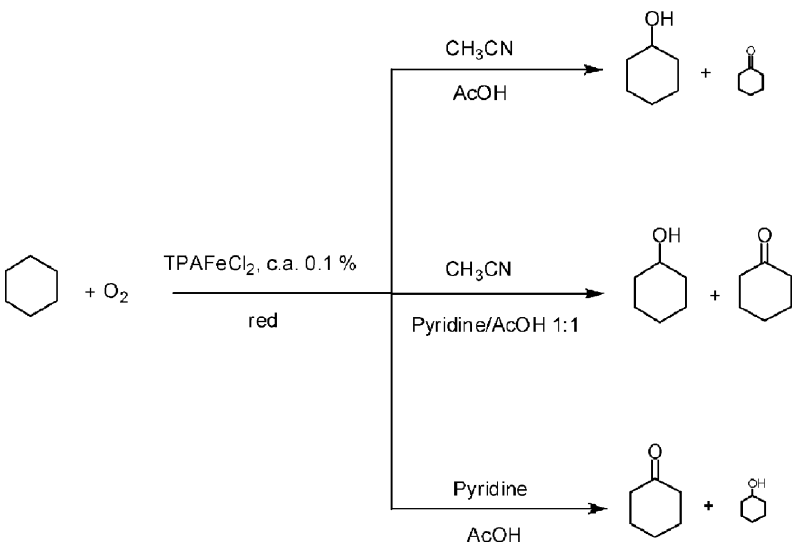

Scheme 3 Changing the solvent from acetonitrile to pyridine dramatically affects the conversion rate and distribution of the reaction products.

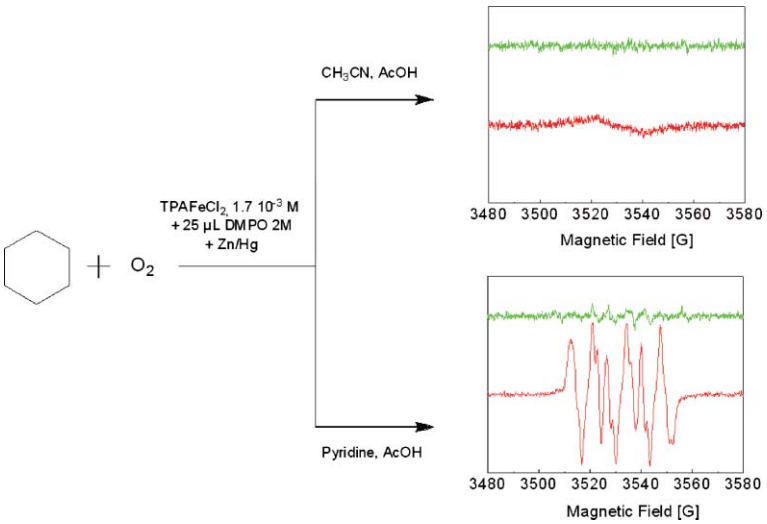

Scheme 4 Room temperature EPR spectra obtained when the reaction was carried out in the presence of DMPO as a spin trap. DMPO : complex ratio 50 : 3. Experiments were performed prior (green trace) and following (red trace) the oxygen bubbling.

we did not expect to detect the presence of such species in pyridine, we were not surprised to miss them in acetonitrile either, since they are known to be unstable in these conditions.[45]

3. Discussion

Coordination chemistry

We have already reported the structural characterization of a series of $FeCl_2$ complexes with fluorine-[18,22] and methyl-[41] α-substituted tripods in the tris(2-pyridylmethyl)amine family of ligands. Monosubstitution at the α position generally affords six-coordinate iron centres, whereas trisubstitution leads to hypodentate coordination of the tripod, the geometry becoming trigonal bipyramidal (TBP). The molecular structures of $Cl_1TPAFeCl_2$ and $Cl_3TPAFeCl_2$ exhibit comparable features to those derived from complexes with mono- and trisubstituted tripods. With α-disubstituted tripods, we reported that a progressive increase of the size of the substituent causes, when steric hindrance remains moderate (fluoro-substituted tripods), *trans*-equatorial distortion within the coordination polyhedron.[18] For more consequent repulsions (methyl-substituted tripods), there is a noticeable elongation of the metal to pyridine distances.[41] In extreme conditions, with bulky substituents such as in $Br_2TPAFeCl_2$, this elongation becomes high enough to unhook one of the substituted pyridines and decoordination occurs, leaving the metal centre in a TBP geometry.[25] In the solid state the $Cl_2TPAFeCl_2$ complex lies in the intermediate situation, with Fe–N4 = 2.50 Å, the pyridine remains coordinated, yet weakly bound and more flexible. As a mechanical effect, the equatorial Cl1, Cl2, N1 and N2 atoms are almost coplanar.

A careful analysis of the spectroscopic data allows an estimation of the geometry in solution. Narrow signals in the ^1H NMR spectra and a pronounced MLCT absorption in the UV-vis spectroscopy generally reflect six-coordination of the tripod in a pseudo-octahedral geometry.[25,41] Switching to TBP geometry induces a broadening of the signals in the ^1H NMR spectra and a noticeable (sometimes dramatic) decrease in the intensity of the MLCT signals. With $Cl_1TPAFeCl_2$ and $Cl_3TPAFeCl_2$, there is no doubt upon examination of the spectroscopic data that the geometry as seen in the solid state is retained in solution.

The case of $Cl_2TPAFeCl_2$ is different, the ^1H NMR and UV-vis data are qualitatively identical to those already reported for $Br_2TPAFeCl_2$, in which the TBP geometry is retained in solution. Thus two distinct forms are found, in the solid state and in solution, respectively, as drawn in Scheme 5.

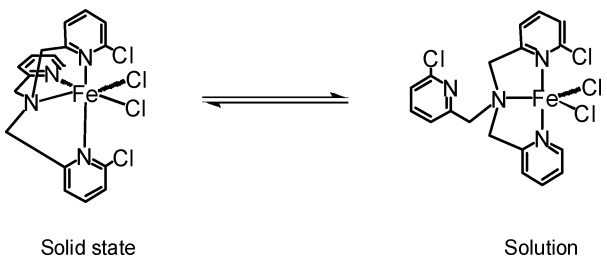

Scheme 5 Solid state *vs.* solution coordination equilibrium in $Cl_2TPAFeCl_2$.

In the present study, the $Fe(OTf)_2$ complexes were prepared in view of their further reaction with hydrogen peroxide, for the purpose of comparison with our O_2–ZnHg system. The preparation of such compounds does not lead to any particular comment. We used relatively hindered substituents in the α-position and, as expected in such cases,[29] we obtain high-spin Fe(II) compounds, with paramagnetic signals in the ^1H NMR spectra supporting pseudo-octahedral geometries. Dissolution of the $Fe(OTf)_2$ complexes with tripodal ligands in acetonitrile generally affords dicationic species, resulting from the displacement of the triflate ions by acetonitrile. The probe to confirm this hypothesis is ^{19}F NMR spectroscopy, a well documented technique with respect to the coordination of triflate ions to paramagnetic iron centres.[30,42,43] With chemicals shifts in the range −72 to −74 ppm and a maximum signal broadening of 230 Hz for the Cl_3TPA ligand, it seems obvious that the triflate ions definitely remain

uncoordinated. Thus, in CH_3CN solution, these complexes can be formulated as $[Cl_nTPAFe(CH_3CN)_2](OTf)_2$.

Reactivity with H_2O_2

The reactivity of the $[TPAFeCl_2]^+$ cation *vs.* H_2O_2 in the presence of cyclooctane has already been reported.[44] With respect to the present work, there was a significant difference in the oxidation state of the iron centre, which was +3 in that case, and the use of pyridine, chosen because of its efficiency as a solvent in the Gif systems. Even so, a lower activity than that observed in the present study was observed. In the present study, we re-investigated the $Fe^{(II)}/H_2O_2$ couple in order to obtain data for comparison purposes with our O_2–ZnHg–AcOH system. The reactivity of the catalytically active systems involving the $Fe^{(II)}/H_2O_2$ couple is very well documented.[10–15,45,46,48] As stated above, in the chemistry of TPA complexes, cyclohexane can be converted into a mixture of cylcohexanol/one with A/K ratios of up to 11.0, using complexes with weakly coordinating counter anions. We chose to use a larger excess of oxidant than is usually reported to improve the number of cycles at the metal site.[47] We checked that the reaction profile remained unchanged when the reaction was carried out under dioxygen, confirming the absence of short-lived radical species in the reaction pathway. We also noted that previous studies reported that γ-nitro substitution of the ligands attached to iron complexes decreased the activity of the catalyst.[32] We followed the H_2O_2 procedure with the $Cl_nTPAFeCl_2$ and $Cl_nTPA(OTf)_2$ series of complexes and found the same trend, *i.e.* a decrease of the activity upon substitution, with a slight increase of the A/K ratio when using a monosubstituted ligand. Finally, we found that the efficiency was slightly better, yet not substantially different, with triflate-coordinated complexes than with the $FeCl_2$ complexes. A dramatic selectivity effect when switching from chloride ligated complexes to bis-acetonitrile dications has already been reported.[48] In the present case, this effect is weak. At this point, it is useful to remember that the decrease in selectivity as a direct consequence of increasing the amount of oxidant is well known and has already been reported.[45] Thus, the moderate difference in activity of both complexes certainly reflects the use of large amounts of oxidant.

Reactivity with O_2

Complexes alone. We previously reported that $FeCl_2$ complexes within the series of α-fluoro substituted tripods react with O_2 to afford diferric μ-oxo species and that subsequent recovery of the ferrous compound can be achieved by reduction with zinc amalgam, allowing several oxygenation–reduction cycles to be completed.[18,21] Thus, although sensitive, our complexes turned out not to decompose under oxygen. For six-coordinate complexes, we reported that O_2 does coordinate to the metal centre, through a mechanism involving initial dissociation of one of the Fe–Cl bonds.[19] The reactivity *vs.* dioxygen could be addressed by monitoring the formation of these μ-oxo dimers at a single wavelength.[18] From kinetic analysis, two distinguishable steps with rate constants termed k_1 and k_2, respectively, could be deduced and these were used to appreciate the oxygen-sensitivity of our complexes. The oxygenation of $Cl_1TPAFeCl_2$ was monitored and complete conversion was observed within 36 h. The values of the two-step kinetic constants k_1 and k_2 lie within a comparable order of magnitude to those found for the $F_1TPAFeCl_2$ and $TPAFeCl_2$ complexes, indicating smooth oxygen sensitivity in solution. In the case of $Cl_2TPAFeCl_2$ and $Cl_3TPAFeCl_2$, the reaction was found to be complete over 6 and 3 h respectively, following a multi step process. The faster conversion of these complexes is attributed to their TBP (*i.e.* coordinatively unsaturated) geometry. We thus have a series of complexes that display oxygen sensitivity in the order $TPAFeCl_2 \approx Cl_1TPAFeCl_2 \ll Cl_2TPAFeCl_2 \approx Cl_3TPAFeCl_2$.

In dry CH_3CN solution, the $Fe(OTf)_2$ complexes turned out to be spectroscopically insensitive to dioxygen. Absolutely no spectroscopic changes (either in UV-vis or ^1H NMR) could be detected upon long-time exposure to O_2.[49] For this reason, the reactivity of the triflate complexes in the alkane oxidation by the O_2–ZnHg system will not be described in the present report.

We wish to come back to the fact that the formation of μ-oxo diferric compounds from O_2 and Fe(II) complexes is a general reaction and that free access of O_2 to the metal centre, allowing its coordination to iron, is crucial.[19,21] In former reports, we adapted the scheme published in the late 70's by porphyrin chemists, the reaction pathway known as "autoxidation of iron porphyrins".[18,22,50] The four key steps in this mechanism, displayed in Scheme 6, are: (i) the formation of the iron-dioxygen adduct,

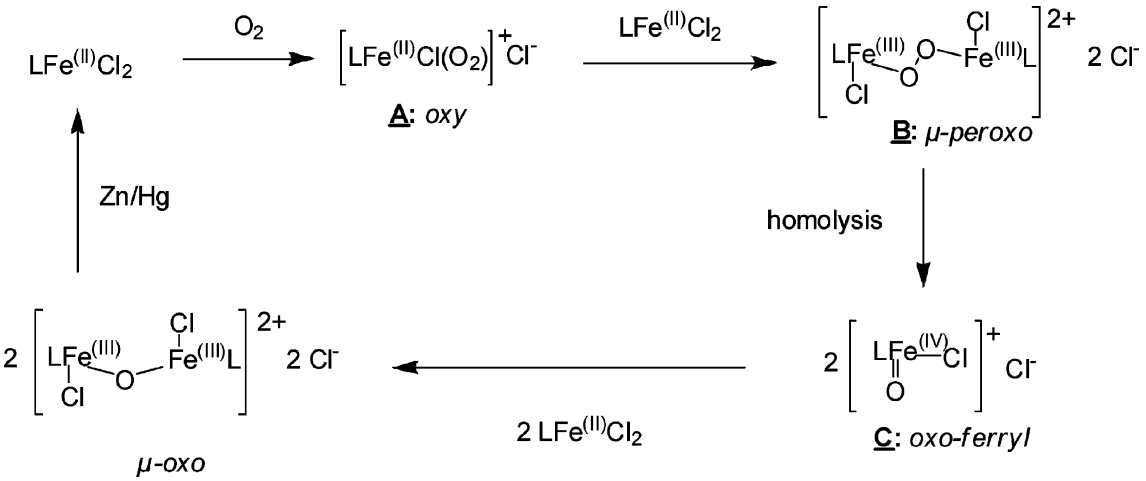

Scheme 6 Adaptation of the Autoxidation Mechanism to the chemistry of O_2-sensitive TPA complexes.[22,50]

termed "oxy" intermediate **A**, (ii) the formation of the μ-peroxo diferric species **B** by reaction of the oxy intermediate with 1 equiv. of the ferrous precursor, (iii) the cleavage of the O–O bond in the μ-peroxo diferric to afford 2 equiv. of Fe(IV)═O, termed oxo ferryl species **C** and (iv) the reaction of one oxo ferryl with one ferrous precursor to afford the final μ-oxo diferric compound.

Complex TPAFeCl$_2$ with cyclohexane, Zn/Hg and the role of protons. Among all the complexes studied, only the parent TPAFeCl$_2$ complex and Cl$_1$TPAFeCl$_2$ exhibited a noticeable reactivity (a likely explanation for this will be given below). We thus focused our studies on the behaviour of the parent TPAFeCl$_2$.

The possible involvement of a potentially reactive species prompted us to investigate the reaction in the strict respect of the conditions depicted in Scheme 6. Since no conversion was observed, it appeared that this scheme does not account for the formation of the reaction product.

The addition of acetic acid turned out to be crucial in order to observe the conversion of cyclohexane into alcohol and ketone, yet with a weak efficiency in CH_3CN. The 3.1 A/K ratio suggests a similar mechanism to that postulated in the reaction of triflato Fe(II) TPA complexes with hydrogen peroxide.[46] The selectivity in the oxidation of adamantane, although not as high as that observed from triflato Fe(II) complexes and hydrogen peroxide,[46] is higher than that generally observed in free-radical oxidation processes,[33–35] in line with a weakly selective metal oxo-process.[35] The fact that cyclohexanol is not oxidized under the same experimental conditions indicates that the ketone is not formed by oxidation of the alcohol.

In order to compare our reaction conditions with those of the "Gif system",[1,44,52] we replaced acetonitrile with pyridine. A drastic modification of the reaction course was observed, with an increase of the activity and a selectivity now being driven towards the formation of the ketone form (A/K = 0.15). The same effect was observed in the oxidation of adamantane, with a 3°/2° ratio more than three-fold less than that in acetonitrile. This suggests the occurrence of a radical-based mechanism in pyridine.

At this point, the question of what kind of species could be proton-sensitive can be raised.

(i) The mesomeric form of a dioxygen adduct **A** can be written as a ferric superoxide species according to Scheme 7:

The presence of a source of protons in the medium would very likely result in the protonation of the superoxide ion to afford the $HO_2^{\bullet}$ radical, leading to radical-based chemistry.

ii) The transient μ-peroxo species **B** for which mesomeric forms can be drawn as shown in Scheme 8 is also likely to be protonated to yield the hydroperoxide **D**.

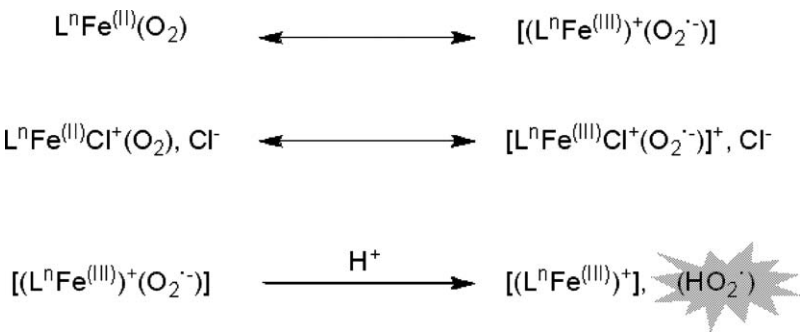

Scheme 7 The "oxy-Fe(II)" forms can also be described as "superoxo-Fe(III) species", yielding the $HO_2^{\bullet}$ radical in protic media.

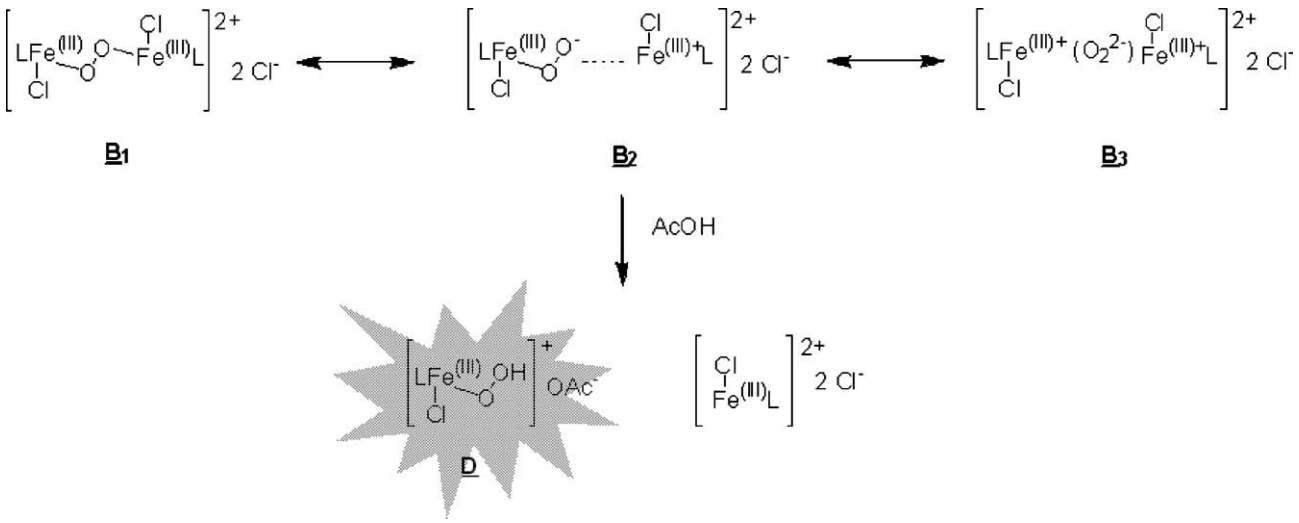

Scheme 8 The μ-peroxo diferric species can also be described as "peroxoferric-Fe(III) species", yielding two species upon protonation: a hydroperoxoferric compound **D** and a ferric derivative.

Ferric hydroperoxide species **D** are known in the literature. They are generally obtained from H_2O_2 and Fe(II) or Fe(III) complexes and can sometimes be spectroscopically detected at low temperature.[11,31,45,46,51] Considering molecular oxygen, two recent reports describe the spectroscopic characterization of such species from O_2, protons and external reducing agents.[23,24] Thus, protonation of **B** to yield **D** (and some ferric compound left over) seems to be a credible hypothesis.

Interestingly, the mesomeric form of the ferric hydroperoxide species **D** can be written as a ferric compound plus the first deprotonated form of hydrogen peroxide according to:

$$L^nFe^{(III)}(O_2H) \leftrightarrow [(L^nFe^{(III)})^+, (HO_2^-)]$$

The chemistry of hydrogen peroxide has been the subject of many investigations in the past.[53] At this stage of the discussion, it is now essential to remember that in pyridine, not in acetonitrile, the hydroperoxide anion was, more than thirty years ago,[54] shown to decompose into $O2^{\bullet -}$ and $HO^{\bullet}$ according to:

$$HO_2^- + H_2O_2 \xrightarrow{\text{pyridine}} O_2^{\bullet -} + OH^{\bullet} + H_2O$$

In this work, hydrogen peroxide was deprotonated by a strong base.

Coming back to the present case, our reaction medium contains some peroxide and hydroperoxide anions, and possibly some hydrogen peroxide, all resulting from the reduction of the coordinated O_2 in a protic medium. In pyridine, it is therefore not surprising to observe a radical pathway, as previously reported in early works,[54] leading to the formation of ketone as the main reaction product. This means our results are perfectly in line with the experimental observation reported more than thirty years ago.[54]

Mechanistic considerations. In the present study, the main result concerns O-atom transfer from O_2 to an inactive substrate and a dramatic solvent effect on the product profile. Scheme 9 depicts the possible mechanistic pathways that are consistent with our experimental observations.

1. In the absence of protons, nothing other than the formation of the diferric μ-oxo species happens (pathway I: deactivation by formation of μ-oxo), in spite of the involvement of a potentially reactive oxo-ferryl species **C**.

2. We show that even if the efficiency is much lower, the reactivity of our AcOH–O_2–ZnHg–$Fe^{(II)}$–acetonitrile system qualitatively parallels that observed with hydrogen peroxide, *i.e.* cyclohexane is converted into cyclohexanol and some cyclohexanone. This strongly suggests the involvement of a similar active species **D** in both conditions (II: peroxide biomimetic pathway).

3. A gradual increase in the amount of added pyridine results in pulling the reaction towards the formation of radicals. Acetic acid is gradually converted into pyridinium acetate as a mild source of protons,[55,56] providing stable radicals.[54] As a consequence: (1) the activity increases (by up to 7 fold when pyridine is the solvent) and (2) the selectivity is driven towards the formation of ketone as the main product. This reaction pathway (pathway III, radical pathway) is obviously different from that mentioned for acetonitrile.

Finally, the radical-based character of the reaction in pyridine could definitely be established by our spin trapping experiments. The striking point came from the spectroscopic comparison between the two reaction conditions: significant amounts of the

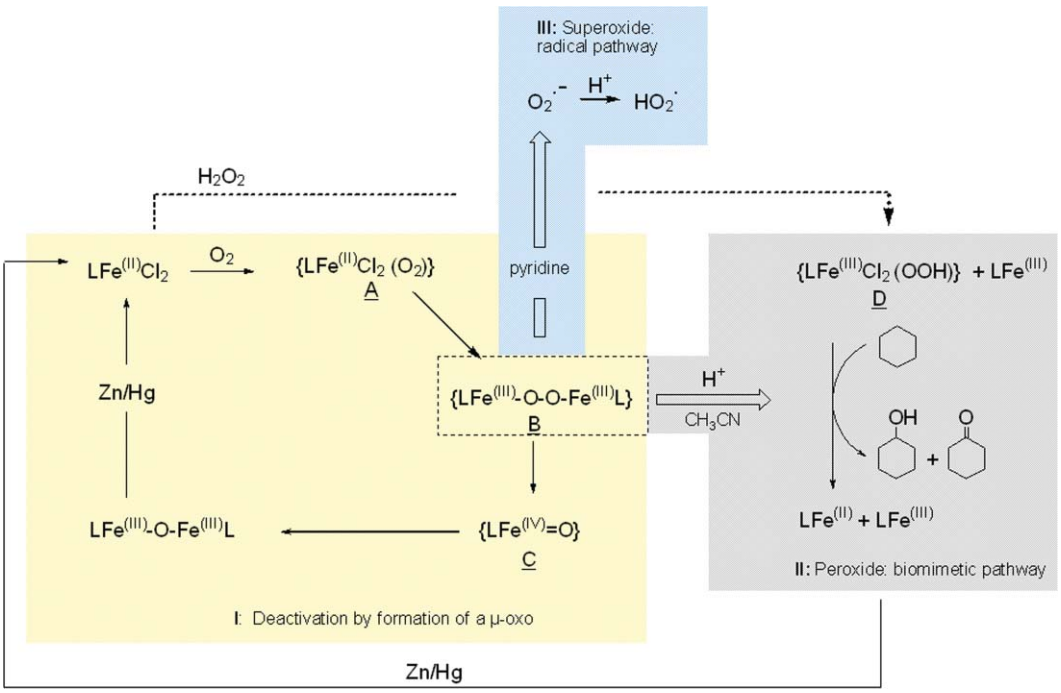

Scheme 9 Autoxidation of ferrous compounds in the absence of protons (in yellow) and the pathways leading to radical chemistry and the conversion of cyclohexane into cyclohexanol/one in the presence of protons.

superoxide anion $O_2^{\bullet -}$ (as its protonated $HO_2^{\bullet}$form) and $OH^{\bullet}$ radical could be trapped by DMPO in pyridine only. On the other hand, the use of acetonitrile as a solvent did not enable the detection of any paramagnetic species, neither oxygenated nor ferric hydroperoxide. The lack of the signature of this latter product was attributed to the instability of such species in our reaction conditions.[45]

In light of these considerations, we believe that we observe here a versatile acid–base chemistry involving two forms of oxygen-active species. The doubly reduced form of dioxygen within the μ-peroxo transient is protonated. In acetonitrile, the main process[58] follows a metal–oxo based pathway. In pyridine, radicals are produced, leading to a different reaction course. This interpretation is illustrated in Scheme 10.

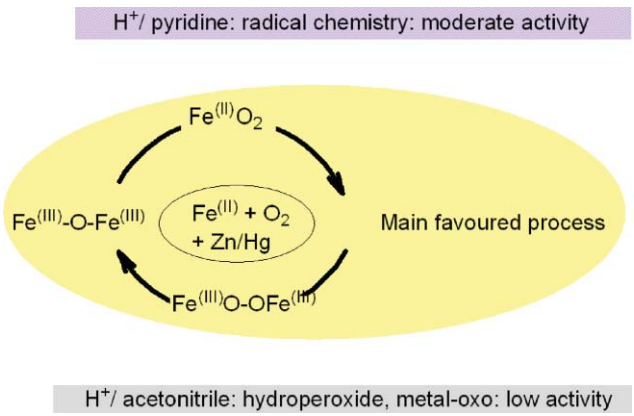

Scheme 10 Schematic interpretation of the experimental results observed in the present study.

Comparison within the series of $Cl_nTPAFeCl_2$ complexes. Coming back to Table 2, it is obvious that the efficiency of the O_2–ZnHg–AcOH system in acetonitrile remains weak. This might be due to the fact that formation of the μ-oxo species is the thermodynamically favoured reaction (the main favoured process in Scheme 10). This also explains why the most oxygen-sensitive five-coordinated complexes, the $Cl_2TPAFeCl_2$ and $Cl_3TPAFeCl_2$ complexes, exhibit a poor reactivity in the presence of a substrate, they simply convert too fast into the μ-oxo species. Thus, optimization of the system would require decreasing the ability of the ferrous compounds to form μ-oxo compounds, while maintaining a good activity *vs.* dioxygen. Efforts are ongoing in this direction in our laboratory.

4. Conclusion

Our first idea when we started this work was to exploit the oxygen sensitivity of the $FeCl_2$ complexes within a series of α-chloro-substituted TPA-type ligands, aiming to study the feasibility of oxygen-transfer reactions on inactive substrates. The full characterization of all complexes with the generic $Cl_nTPAFeCl_2$ formula has now become available. As expected, we found that the effect of α-chlorination was to increase the oxygen sensitivity with a maximum effect for complexes with trigonal bipyramidal geometry in solution. We then observed that the complexes with a moderate sensitivity allow oxygen atom transfer from O_2 to cyclohexane in the presence of protons and a reducing agent, in a similar fashion to that reported when hydroperoxides and iron complexes are reacted together. Although very limited in efficiency, this transformation represents one of the very few functional examples of C–H hydroxylation of an inert substrate by a well-defined mononuclear non-porphyrinic iron complex in mild conditions.

Keeping in mind the Gif chemistry, we then decided to use the $TPAFeCl_2$ complex as a tool to compare our approach with that previously reported in the former abundant literature and worked in similar conditions as those reported in the Gif[IV] chemistry. Following these conditions, we found a completely different reactivity, with enhanced efficiency but opposite selectivity, the ketone being obtained as the main product within a radical-based reaction mechanism.

The radical process[57] or biomimetic pathway dichotomy has been the subject of many controversies in the past. The first outcome of the present work is to demonstrate that the coordination of O_2 is a pre-requisite to promote such conversions. The second one is the illustration of the chemical versatility of active sites, in the present case an oxygen-coordinated metal centre, in an *a priori* simple process. Future development of this work will involve optimization of the balance between the efficiency in reactivity and ease of use, in other words the "operational stability", of simple ferrous complexes.

5. Experimental

General considerations

Chemicals were purchased from Aldrich Chemicals and used as received. The DPA bis(2-pyridylmethyl)amine and TPA ligands were prepared according to published procedures: G. Andregg; F. Wenk, *Helv. Chim. Acta*, 1967, **50**, 2330; M. S. Nelson, J. Rodgers, *J. Chem. Soc. A*, 1968, 272; M. M. Da Mota, J. Rodgers, S. M. Nelson, *J. Chem. Soc. A*, 1969, 2036–2044. All the solvents used during the metallation reactions, work-up and reactivity were distilled and dried according to W. L. F. Armarego.; D. D. Perrin, *Purification of Laboratory Chemicals*, 4th ed.; Pergamon Press, Oxford, 1997.

Analytical anhydrous $FeCl_2$ was obtained as a white powder by reacting iron powder (ACS grade) with hydrochloric acid in the presence of methanol under an argon atmosphere. Preparation and handling of all the compounds was performed under an argon atmosphere using Schlenk technique, following standard procedures. The purity of the dry dioxygen was 99.999% (grade 5). Zinc amalgam was prepared as follows: a mixture of 200 g of mercury, 2 g of zinc powder and 100 cm^3 of 25% aqueous sulfuric acid were stirred until no zinc powder was visible. The acidic phase was removed and the amalgam was thoroughly washed with distilled water until a neutral pH was reached. 5 cm^3 of fresh mercury was added. The resulting amalgam was filtered on a paper skimmer and washed twice with dry THF. It was then left under primary vacuum overnight. Elemental analyses were carried out by the Service de Microanalyse de l'Institut de Chimie de Strasbourg, Université de Strasbourg, France. Mass spectroscopy experiments were carried out by the Service Commun de Spectrometrie de Masse de l'Institut de Chimie de Strasbourg. The structural determinations were carried out by the Service

de Diffraction des Rayons X, Institut de Chimie, Université de Strasbourg.

Physical methods

^{1}H NMR data were recorded in CD_3CN for the complexes and $CDCl_3$ for the ligands at ambient temperature on a Bruker AC 300 spectrometer at 1300 MHz using the residual signal of CD_2HCN ($CHCl_3$) as a reference for calibration. The UV-vis spectra were recorded on a Varian Cary 05 E UV-VIS NIR spectrophotometer equipped with an Oxford instrument DN1704 cryostat, using optically transparent schlenck cells. The kinetic data were analysed with the commercial software IGOR pro version 4.0.8.0, Wavemetrics inc., USA, 2003. Conductivity measurements were carried out under argon at 20 °C with a CDM 210 Radiometer Copenhagen Conductivity Meter, using a Tacussel CDC745-9 electrode. Cyclic voltammetry measurements were obtained from a PAR 173A potentiostat in a 0.1 M acetonitrile solution of $TBAPF_6$ (supporting electrolyte), using platinum electrodes and saturated calomel electrode as reference. For each measurement, the potential was checked by addition of a small amount of ferrocene (Fc/Fc^+ = 0.380 v/SCE) in the cell. Gas-phase chromatography was performed on a Varian GC3900 apparatus, equipped with a capillary column (CP-Wax 52 CB, 15 m × 0.25 mm × 0.39 mm), using a Flame Ionization Detector and helium as the carrier gas. A continuous-wave EMXplus X-band spectrometer (Bruker Biospin GmbH, Germany) equipped with a high sensitivity resonator (4119HS-W1, Bruker) was used for acquiring the EPR spectra.

Synthesis of ligands

2-chloro-6-bromomethyl pyridine. To a solution of 4 g, (30 mmol) of 2-chloro-6-methyl pyridine in 200 mL of CCl_4 were added 6 g (30 mmol) of N-bromosuccinimide and 300 mg (1.25 mmol) of dibenzoyl peroxide. The medium was refluxed for 5 h, then cooled to room temperature. The solvent was evaporated, and the residue extracted with toluene. After filtration, the toluene solution was washed with water and dried on $MgSO_4$. The concentrated toluene phase was deposited at the top of a chromatography column mounted with silica gel and toluene. Elution using toluene afforded the desired compound as the third fraction. 2.22 g (10 mmol) of a pale white solid were obtained, corresponding to a 34% yield of 2-chloro 6-bromomethyl pyridine.

^{1}H NMR, $CDCl_3$, δ, ppm: 7.66 (t, γ-C*H*, 1H), 7.38, (d, β-C*H*, 1H), 7.25 (d, β-C*H*, 1H); 4.48, (s, CH_2, 2H)

Cl_1TPA = (2-chloro-6-pyridylmethyl)bis(2-pyridylmethyl)amine. To a solution of 0.5 g (2.42 mmol) of 2-chloro-6-bromomethyl pyridine in 200 cm^3 of EtOH, were added 0.48 g (2.41 mmol) of bis(2-pyridylmethyl)amine and 0.85 g (0.01 mmol) of $NaHCO_3$. The reaction mixture was refluxed over 16 h. Afterwards, the solvent was evaporated to dryness. After water was added, the mixture was extracted several times with CH_2Cl_2, and the combined organic phases washed with water and then dried over $MgSO_4$. Addition of pentane to the concentrated organic phases allowed precipitation of a white solid, which was filtered and dried under vacuum. The yield was 0.34 g (43.5%).

^{1}H NMR, $CDCl_3$, δ, ppm: 8.54 (m, α-CH_{arom}, 2H); 7.60 (m, CH_{arom}, 6H); –7.15 (m, CH_{arom}, 3 H); 3.89, (s, CH_2, 4H); 3.87 (s, CH_2, 2H).

^{13}C NMR, $CDCl_3$, δ, ppm: 160.6 (*ipso* C_{arom} substPy); 159.0 (*ipso* C_{arom} unsubstPy); 150.6 (*ipso* ClC_{arom}Py); 149.1, 136.4, 123.0 and 122.0 (CH_{arom} unsubstPy); 139.0, 122.4, 121.2 (CH_{arom} substPy); 60.1 (CH_2 unsubstPy); 59.5 (CH_2°substPy).

Elemental analysis for $C_{18}H_{17}N_4Cl$: calc. (%): C 66.5, H 5.2, N 17.2. Found (%): C 66.0, H 5.4, N 17.0.

Cl_2TPA = bis (2-chloro-6-pyridylmethyl)(2-pyridylmethyl)amine. To a solution of 1.5 g (7.3 mmol) of 2-chloro-6-bromomethyl pyridine in 200 cm^3 of EtOH were added 0.39 g (3.6 mmol) of picolylamine and 1.5 g (14.15 mmol) of Na_2CO_3. The reaction mixture was refluxed over 16 h. Afterward, the solvent was evaporated to dryness. After water was added, the mixture was extracted several times with CH_2Cl_2, and the combined organic phases washed with water then dried over $MgSO_4$. Addition of pentane to the concentrated organic phases yielded 0.59 g (40%) of a white solid.

^{1}H NMR, $CDCl_3$, δ, ppm: 8.54 (m, α-CH_{arom}, 1H); 7.68–7.50 (m, CH_{arom}, 6H); 7.17 (m, CH_{arom}, 3 H); 3.89, (s, CH_2, 2H); 3.87 (s, CH_2, 4H).

^{13}C NMR, $CDCl_3$, δ, ppm: 160.3 (*ipso* C_{arom} substPy); 158.8 (*ipso* C_{arom} unsubstPy); 150.6 (*ipso* ClC_{arom} Py); 149.2, 136.4, 123.1 and 122.1 (CH_{arom} unsubstPy); 139.0, 122.5, 121 (CH_{arom} substPy); 60.1 (CH_2 unsubstPy); 59.5 (CH_2 substPy).

Elemental analysis for $C_{18}H_{16}N_4Cl_2$: calc. (%): C 60.1, H 4.4, N 15.6. Found (%): C 59.6, H 4.9, N 15.3.

Cl_3TPA = tris (2-chloro-6-pyridylmethyl)amine. 1.5 g (7.3 mmol) of 2-chloro-6-bromomethyl pyridine were suspended with NH_4Cl (145 mg, 2.43 mmol) in a mixture of THF and H_2O 90 : 10 (150 mL). The pH was adjusted to 10 by addition of aqueous NaOH. The resulting medium was stirred for 4 d at room temperature in a tightly closed flask. After THF evaporation, the reaction mixture was then poured into CH_2Cl_2 and the organic phase separated, washed with water and then dried by $MgSO_4$. Addition of cold hexane to the concentrated organic phases yielded 0.22 g (23%) of a white solid.

^{1}H NMR, $CDCl_3$, δ, ppm: 7.62 (t, γ-CH_{arom}, 3H); 7.50 (d, β-CH_{arom}, 3H); 7.19 (d, β-CH_{arom}, 3 H); 3.87 (s, CH_2, 6H).

^{13}C NMR, $CDCl_3$, δ, ppm: 160.0 (*ipso* C_{arom} substPy); 147.2 (*ipso* ClC_{arom} Py); 140.2, 125.0, 122.1 (CH_{arom} substPy); 50.6 (CH_2 substPy).

Mass spectroscopy: ES$^+$, *m*/*z*: 393.0347 (Cl_3TPAH^+), 395.0318 (Cl_3TPAH^+), corresponding to the two isotopes of Cl of $C_{18}H_{15}Cl_3N_4H^+$.

Elemental analysis for $C_{18}H_{15}N_4Cl_3$: calc. (%): C 54.9, H 3.8, N 14.2. Found (%): C 54.3, H 4.1, N 14.6.

Preparation of the complexes

Preparation of the $FeCl_2$ complexes. Details are given for $Cl_1TPAFeCl_2$, but the following procedure applies to all complexes: 150 mg (0.46 mmol) of free Cl_1TPA were dissolved in a schlenk tube containing 20 mL of dry and degassed THF. 55 mg (0.43 mmol) of anhydrous $FeCl_2$ was dissolved in a second schlenck tube containing 10 mL of dry and degassed THF. The solution of $FeCl_2$ was transferred under argon in the schlenck containing the

ligand, and the medium was stirred overnight. The solvent was then evaporated to dryness, and the compound was extracted with dry and degassed CH_3CN, filtered under inert atmosphere and concentrated. Addition of diethyl ether afforded a yellow solid, which was washed thoroughly with this solvent, prior to be dried under vacuum. 180 mg (86%) of $Cl_1TPAFeCl_2$ with good analytical and spectroscopic data could be obtained.

Preparation of the Fe(OTf)$_2$ complexes. Details are given for $TPAFe(OTf)_2$, but the following procedure applies to all complexes: 150 mg (0.51 mmol) of free TPA were dissolved in a schlenk tube containing 20 mL of dry and degassed THF. 204 mg (0.46 mmol) of anhydrous $Fe(OTf)_2$ was dissolved in a second schlenck tube containing 10 mL of dry and degassed THF. The solution of $Fe(OTf)_2$ was transferred under argon in the schlenck containing the ligand, and the medium was stirred overnight. The solvent was then evaporated to dryness, and the compound was extracted with dry and degassed CH_3CN, filtered under inert atmosphere and concentrated. Addition of diethyl ether afforded a brownish-red solid, which was washed thoroughly with this solvent, prior to be dried under vacuum. When dry, the compound appears as a dark-red solid. 280 mg (84%) of $TPAFe(OTf)_2$ with a ^{1}H NMR trace identical to that reported in: A. Diebold; K. S. Hagen, *Inorg. Chem.*, 1998, **37**, 215–223.

Elemental analysis for $Cl_1TPAFe(OTf)_2{\cdot}H_2O$, $C_{20}H_{19}N_4ClF_6S_2O_7Fe$: calc. (%): C 34.4, H 2.7, N 8.0. Found (%): C 34.3, H 3.0, N 8.1.

Elemental analysis for $Cl_2TPAFe(OTf)_2{\cdot}4H_2O$, $C_{20}H_{24}N_4Cl_2F_6S_2O_{10}Fe$: calc. (%): C 30.6, H 3.1, N 7.1. Found (%): C 30.7, H 3.1, N 7.0

Elemental analysis for $Cl_3TPAFe(OTf)_2$: this compound is very hygroscopic and different samples of the same batch gave non reproducible values. Best result obtained for $Cl_2TPAFe(OTf)_2{\cdot}8H_2O$, $C_{20}H_{31}N_4Cl_3F_6S_2O_{14}Fe$: calc. (%): C 27.1, H 3.5, N 6.3. Found (%): C 26.8, H 2.9, N 5.9

In complexes with $Cl_{1-3}TPA$ ligands, paramagnetic ^{1}H and ^{19}F NMR data were obtained (all traces are given in the ESI†). In the ^{1}H NMR spectra, all the complexes display broadened and shifted signals in line with a high-spin state for the iron centre. For the triflate complexes, all the ^{19}F NMR data support the presence of uncoordinated triflate ions in a CD_3CN solution, although minor broadening may arise from a limited dynamic exchange process in solution.

Cl$_1$FeCl$_2$. ^{1}H NMR spectrum in CD_3CN, R.T. δ, ppm CHD_2CN: 125: α; 63, 55, 21: CH_2; 52, 44: β,β′ unsubst. Py; 45, 31: β,β′subst. Py; 17: γ, unsubst. Py; 14: γ, subst. Py.

Cl$_1$Fe(OTf)$_2$. ^{1}H NMR spectrum in CD_3CN, R.T. δ, ppm CHD_2CN: 105: α; 88, 83, 37: CH_2; 52, 54: β,β′ unsubst. Py; 56, 46: β,β′subst. Py; –4: γ, unsubst. Py; –2: γ, subst. Py.

^{19}F NMR, δ: –72.1 ppm ($\Delta\nu_{1/2}$ = 35 Hz).

Cl$_2$FeCl$_2$. ^{1}H NMR spectrum in CD_3CN, R.T. δ, ppm CHD_2CN: CH_2; 52, 44: β,β′ unsubst. Py; 45, 31: β,β′subst. Py; 17: γ, unsubst. Py; 14: γ, subst. Py.

Cl$_2$Fe(OTf)$_2$. ^{1}H NMR spectrum in CD_3CN, R.T. δ, ppm CHD_2CN: 99, 80, 58: CH_2; 64, 44: β,β′ subst. Py; 57, 55: β,β′unsubst. Py; 0: γ, subst. Py; –4: γ, unsubst. Py.

^{19}F NMR, δ: –74.1 ppm ($\Delta\nu_{1/2}$ = 90 Hz).

Cl$_3$FeCl$_2$. ^{1}H NMR spectrum in CD_3CN, R.T. δ, ppm CHD_2CN: extremely broad signals over 70–30 ppm, in line with a high-spin Fe(II) complex in trigonal bipyramidal geometry (ref. 14 and 18)

Cl$_3$Fe(OTf)$_2$. ^{1}H NMR spectrum in CD_3CN, R.T. δ, ppm CHD_2CN: 40, 60 and broad and poorly defined signals between 5 and 0 ppm.

^{19}F NMR, δ: –74.2 ppm ($\Delta\nu_{1/2}$ = 230 Hz).

Single-crystal X-ray data

Crystallization of Cl$_1$TPAFeCl$_2$. A solution of $Cl_1TPAFeCl_2$ in dry CH_2Cl_2 was layered with dry and degassed diethyl ether. Orange single crystals were easily obtained over 2–3 d of diffusion time under strict anaerobic conditions.

Crystal data for $Cl_1TPAFeCl_2$. Orange crystals, 0.40 × 0.38 × 0.35 mm^3. C18 H17 Cl3 Fe N4, CH2Cl2, M = 536.48 g mol^{-1}. Monoclinic, space group $P2_1/c$, a = 10.2750(4), b = 13.5295(5), c = 16.2447(4) Å, β = 94.919(2)°, V = 2249.95(13) Å^3, ρ_c = 1.584 g cm^{-3}, Z = 4, 0.998 < θ < 30.034. Of 6556 total reflections, 4551 were considered to be observed [$I > 2\sigma(I)$], with 262 parameters. Final results: R = 0.0486 and R_w = 0.1437; GOF = 1.081.

Crystalization of Cl$_2$TPAFeCl$_2$. A solution of $Cl_2TPAFeCl_2$ in dry CH_3CN was layered with dry and degassed diethyl ether: yellow single crystals were easily obtained over 2–3 d of diffusion time under strict anaerobic conditions.

Crystal data for $Cl_2TPAFeCl_2$: Yellow crystals, 0.40 × 0.35 × 0.30 mm^3. C18 H16 Cl4 Fe N4, M = 486.00 gmol^{-1}. Monoclinic, space group Cc, a = 9.1920(5), b = 15.5454(10), c = 15.1189(8) Å, β = 106.520(3)°, V = 2071.2(2) Å^3, ρ_c = 1.559 g cm^{-3}, Z = 4, 0.998 < θ < 30.034. Of 4056 total reflections, 3368 were considered to be observed [$I > 2\sigma(I)$], with 244 parameters. Final results: R = 0.0387 and R_w = 0.0956; GOF = 1.017.

Crystalization of Cl$_3$TPAFeCl$_2$. A solution of $Cl_3TPAFeCl_2$ in dry CH_3NO_2 was layered with dry and degassed diethyl ether: yellow single crystals were easily obtained over 2–3 d of diffusion time under strict anaerobic conditions.

Crystal data for $Cl_3TPAFeCl_2$: Yellow crystals, 0.24 × 0.11 × 0.10 mm^3. C18 H15 Cl5 Fe N4, M = 520.44 gmol^{-1}. Triclinic, space group $P\bar{1}$, a = 8.6446(5), b = 11.4985(9), c = 13.3214(9) Å, α = 86.774(3)°, β = 75.367(4)°, γ = 78.051(4)°, V = 1253.42(15) Å^3, ρ_c = 1.379 g cm^{-3}, Z = 2, 0.998 < θ < 27.485. Of 5716 total reflections, 4062 were considered to be observed [$I > 2\sigma(I)$], with 253 parameters. Final results: R = 0.0650 and R_w = 0.1967; GOF = 1.038.

Crystallographic data have been deposited with the CCDC, 751031 ($Cl_1TPAFeCl_2$), 751030 ($Cl_2TPAFeCl_2$) and 751029 ($Cl_3TPAFeCl_2$).

Reactivity studies

1. Reaction conditions for the conversions with Cl$_n$TPAFeCl$_2$/O$_2$/Zn/Hg/CH$_3$CO$_2$H in CH$_3$CN. All reactions were carried out at least five times, yielding reproducible results. Average values of TONs are reported with estimated uncertainties ± 5–8%.

Typical reaction. In a finger-size schlenk tube containing one or two drops of zinc amalgam under argon was transferred a solution

containing 1.2–1.7 mg of complex (1 equiv.) in 2 mL of dry and degassed acetonitrile. 0.35 mL (1100 equiv.) of cyclohexane and 0.05 mL (300 equiv.) of acetic acid were added and the medium was vigorously stirred. Dioxygen was then bubbled in the medium over 5 s and the reaction was kept under O_2 atmosphere for five hours, by connection of the schlenk with a O_2-filled rubber balloon. From yellow at the beginning of the reaction, the colour gradually turned to orange and brown. At the end of the reaction time, the medium consisted of a suspension of a grey solid in a pale brown solution.

At this point, a measured volume of acetophenone was added as an external standard for quantitative calibration, magnet stirring was stopped and the solid deposited down to the bottom of the schlenck. A sample of the liquid suspension was extracted and injected into the GC apparatus.

[Mass balance: the estimated loss of cyclohexane was around 2% upon bubbling O_2 and workup (1080 equiv. of recovered material from 1100 equiv. of reagent)]. Only cyclohexanol (retention time: 6 min at 96 °C) and cyclohexanone (retention time: 4.5 min at 78 °C) were detected (GC [total run time of 20 min] and mass spectroscopy).

Attempts to detect cyclohexyl hydroperoxide: the procedure described by Shul'pin *et al.*[59] was carried out. We found that the reaction profile was not modified upon the addition of PPh_3 to the reaction medium prior to injection into the GC. In fact, this procedure was originally setup for hydroperoxide chemistry. In the present case we work in the presence of molecular oxygen and a reducing agent, which might simply react with any cyclohexyl hydroperoxide if any present.

The reaction was carried out in the absence of zinc amalgam and/or acetic acid, following the same procedure. Only trace amounts of the oxidation products from cyclohexane could then be detected.

2. Reaction conditions for the conversion with $TPAFeCl_2/O_2/Zn/Hg/CH_3CO_2H$/pyridine 1 : 1 in CH_3CN. This reaction was carried out three times yielding reproducible results. Average values of TONs are reported with estimated uncertainties ± 5–8%.

Typical reaction. In a finger-size schlenk tube containing one or two drops of zinc amalgam under argon, was transferred a solution containing 1.2 mg of $TPAFeCl_2$ (1 equiv.) in 2 mL of dry and degassed acetonitrile. 0.35 mL (1100 equiv.) of cyclohexane, 0.05 mL (300 equiv.) of acetic acid and 0.07 mL (300 equiv.) of pyridine were added, and the medium was vigorously stirred. Dioxygen was then bubbled in the medium over 5 s, and the reaction was kept over O_2 atmosphere for five hours, by connection of the schlenk with a O_2-filled rubber balloon. From yellow at the beginning of the reaction, the colour gradually turned to greenish yellow. At the end of the reaction time, medium consisted of a suspension of grey solid into a greenish yellow solution.

At this point, the same analytical procedure as that described in reactivity study 1 was carried out.

3. Reaction conditions for the conversion with $TPAFeCl_2/O_2/Zn/Hg/CH_3CO_2H$ in pyridine. This reaction was carried out at least five times, yielding reproducible results. Average values of TONs are reported with estimated uncertainties ± 5–8%.

Typical reaction. In a finger-size schlenk tube containing one or two drops of zinc amalgam was transferred under argon a solution containing 1.2 mg of $TPAFeCl_2$ (1 equiv.) in 2 mL of degassed pyridine. 0.35 mL (1100 equiv.) of cyclohexane and 0.05 mL (300 equiv.) of acetic acid were added, and the medium was vigorously stirred. Dioxygen was then bubbled in the medium over 5 s, and the reaction was kept under an O_2 atmosphere for five hours, by connection of the schlenk with an O_2-filled rubber balloon. From orange at the beginning of the reaction, the colour gradually turned to yellow. At the end of the reaction time the medium consisted of a suspension of a grey solid in a pale yellow solution.

At this point, the same analytical procedure as that described in reactivity study 1 was carried out.

Attempts to detect cyclohexyl hydroperoxide: the procedure described by Shul'pin[59] *et al.* was carried out. We found that the reaction profile was not modified upon the addition of PPh_3 to the reaction medium prior to injection into the GC. In fact, this procedure was originally setup for hydroperoxide chemistry. In the present case we work in the presence of molecular oxygen and a reducing agent, which might simply react with any cyclohexyl hydroperoxide if any present.

4. Reaction conditions for the adamantane conversion with $TPAFeCl_2/O_2/Zn/Hg/CH_3CO_2H$/in CH_3CN or pyridine. This reaction was carried out three times yielding reproducible results. Average values of TONs are reported with estimated uncertainties ± 5–8%.

Typical reaction. In a finger-size schlenck tube containing one or two drops of zinc amalgam was transferred under argon a solution containing 1.2 mg of $TPAFeCl_2$ (1 equiv.) in 2 mL of degassed CH_3CN or pyridine. 0.45 g (1100 equiv.) of adamantane and 0.05 mL (300 equiv.) of acetic acid were added, and the medium was vigorously stirred. Dioxygen was then bubbled in the medium over 5 s, and the reaction was kept under O_2 atmosphere for five h, by connection of the schlenk with a O_2-filled rubber balloon. From yellow at the beginning of the reaction, the colour gradually turned to pink-beige. At the end of the reaction time the medium consisted of a suspension of a grey solid in a clear pink-beige solution.

At this point, the same analytical procedure as that described in reactivity study 1 was carried out.

5. Attempt to convert cyclohexanol into cyclohexanone with $TPAFeCl_2/O_2/Zn/Hg/CH_3CO_2H$ in CH_3CN. This reaction was carried out three times yielding reproducible results. Average values of TONs are reported with estimated uncertainties ± 5–8%.

The same procedure as that reported with cyclohexane (reactivity study 1) was used, except that cyclohexane was replaced by cyclohexanol. Mass balance and GC analysis revealed that no conversion had occurred.

6. Reaction conditions for the conversion with H_2O_2. All reactions were carried out at least three times, yielding reproducible results. Average values of TONs are reported with estimated uncertainties ± 5–8%.

1. Cl_nTPAFeCl$_2$ complexes: Typical reaction. 2.0 ml of a 2.5 M (5 mmol) H_2O_2 solution (diluted from a 33% aqueous solution) in CH_3CN was delivered by a syringe pump over 4 h 30 min at 25 °C under argon, to a vigorously stirred solution (5 mL) containing Cl_{0-3}TPAFeCl$_2$, (10 μmols) and cyclohexane (5 mmol). At this point, a measured volume of acetophenone was added as an external standard for quantitative calibration, magnet stirring

was stopped and 40 µl of the crude medium were diluted into 1 mL of CH_3CN. A sample of the resulting solution was injected into the GC apparatus.

Another set of experiments was carried out under an atmosphere of dioxygen: O_2 was bubbled during 5 s before the addition of H_2O_2 started. The results were not significantly different.

2. $Cl_nTPAFe(OTf)_2$ complexes: Typical reaction. 2.0 ml of a 2.5 M (5 mmol) H_2O_2 solution (diluted from a 33% aqueous solution) in CH_3CN was delivered by a syringe pump over 4h 30 min at 25 °C under argon, to a vigorously stirred solution (5 mL) containing $Cl_{0-3}TPAFe(OTf)_2$, (10 µmol) and cyclohexane (5 mmol). At this point, a measured volume of acetophenone was added as an external standard for quantitative calibration, magnet stirring was stopped and 40 µL of the crude medium were diluted into 1 mL of CH_3CN. A sample of the resulting solution was injected into the GC apparatus.

7. Spin trapping experiments. In a finger-size schlenck tube containing one or two drops of zinc amalgam was transferred, under argon, a solution containing 1.2 mg of $TPAFeCl_2$ (1 equiv.) in 2 mL of dry and degassed solvent (acetonitrile or pyridine). 0.35 mL (1100 equiv.) of cyclohexane and 0.05 mL (300 equiv.) of acetic acid were added, and the medium was vigorously stirred. 25 µL of a 2 M solution of 5,5-dimethyl-1-pyrroline-*N*-oxide (DMPO, purchased from Sigma Aldrich) in distilled H_2O was added, without further purification. Dioxygen was then bubbled in the medium over 5 s, and the medium was stirred for five min. A glass capillary was then filled with 50 µL of solution, centred in a regular 4 mm OD EPR quartz tube and immediately introduced into the EPR cavity. The principal experimental parameters were: gain 40 dB, modulation amplitude 0.5 to 1 G, microwave power 1.8 mW, time constant 20.48 ms, conversion time 30 to 60.1 ms. The centre field was set to 3532 G, 200 G were swept in 60 s per scan. All experiments were performed at room temperature (295 ± 1 K).

Attempt to trap any ferric hydroperoxide species: the same experimental procedure was applied, the medium being transferred into a 4 mm EPR quartz tube (instead of a capillary) and immediately frozen. The data acquisition were performed at 100 K. No paramagnetic species could be observed under these conditions.

Acknowledgements

The CNRS and UdS are gratefully acknowledged. This work was in part realized when Prof. Rémy Louis was Head Manager of the Institut de Chimie de Strasbourg. We wish to address special thanks to him for his constant support and encouragement. The Conseil Scientifique de l'ULP (now UdS) is acknowledged for specific support no. AO CS ULP 2006.

References

1 D. H. R. Barton, M. J. Gastiger and W. B. Motherwell, *J. Chem. Soc., Chem. Commun.*, 1983, 41–43.
2 P. Stavropoulos, R. Celenligil-Cetin and A. E. Tapper, *Acc. Chem. Res.*, 2001, **34**, 745–752.
3 S. Tanase and E. Bouwman, *Adv. Inorg. Chem.*, 2006, **58**, 29–75.
4 J. Du Bois, T. J. Mizogushi and S. Lipperd, *Coord. Chem. Rev.*, 2000, **200–202**, 443–485.
5 S. V. Kryatov, E. V. Rybak-Akimova and S. Schindler, *Chem. Rev.*, 2005, **105**, 2175–2226.
6 M. Abu-Omar, A. Loaiza and N. Hontzeas, *Chem. Rev.*, 2005, **105**, 2227–2252.
7 E. G. Kovaleva and J. D. Lipscomb, *Nat. Chem. Biol.*, 2008, **4**, 186–193.
8 T. Punniyamurthy, S. Velusamy and J. Iqbal, *Chem. Rev.*, 2005, **105**, 2329–2363.
9 J. A. Labinger, *J. Mol. Catal. A: Chem.*, 2004, **220**, 27–35.
10 M. Costas, K. Chen and L. Que, Jr., *Coord. Chem. Rev.*, 2000, **200–202**, 517–544.
11 M. Costas, M. P. Mehn, M. P. Jensen and L. Que, Jr., *Chem. Rev.*, 2004, **104**, 939–986.
12 M. S. Chen and M. C. White, *Science*, 2007, **318**, 783–787.
13 L. Gomez, I. Garcia – Bosch, A. Company, J. Benet-Buchholtz, A. Polo, X. Sala, X. Ribas and M. Costas, *Angew. Chem., Int. Ed.*, 2009, **48**, 5720–5723.
14 M. S. Chen and M. C. White, *Science*, 2010, **327**, 566–571.
15 V. B. Romakh, B. Therrien, G. Suss-Fink and G. B. Shul'pin, *Inorg. Chem.*, 2007, **46**, 3166–3175.
16 N. Kitajima, M. Ito, H. Fukui and Y. Moro-Oka, *J. Chem. Soc., Chem. Commun.*, 1991, 102–104.
17 N. Raffard-Pons, Y. Moll, F. Banse, K. Miki, M. Nierlich and J.-J. Girerd, *Eur. J. Inorg. Chem.*, 2002, 1941–1944.
18 N. K. Thallaj, O. Rotthaus, L. Benhamou, N. Humbert, M. Elhabiri, M. Lachkar, R. Welter, A.-M. Albrecht-Gary and D. Mandon, *Chem.–Eur. J.*, 2008, **14**, 6742–6753.
19 A. Wane, N. K. Thallaj and D. Mandon, *Chem.–Eur. J.*, 2009, **15**, 10593–10602.
20 A. Machkour, D. Mandon, M. Lachkar and R. Welter, *Eur. J. Inorg. Chem.*, 2005, 158–161.
21 L. Benhamou, A. Machkour, O. Rotthaus, M. Lachkar, R. Welter and D. Mandon, *Inorg. Chem.*, 2009, **48**, 4777–4886.
22 A. Machkour, D. Mandon, M. Lachkar and R. Welter, *Inorg. Chem.*, 2004, **43**, 1545–1550.
23 A. Thibon, J. England, M. Martinho, V. G. Young, J. R. Frisch, R. Guillot, J.-J. Girerd, E. Münck, L. Que, Jr. and F. Banse, *Angew. Chem., Int. Ed.*, 2008, **47**, 7064–7067.
24 S. Hong, Y.-M. Lee, W. Shin, S. Fukuzumi and W. Nam, *J. Am. Chem. Soc.*, 2009, **131**, 13910–13911.
25 D. Mandon, A. Machkour, S. Goetz and R. Welter, *Inorg. Chem.*, 2002, **41**, 5364–5372.
26 A. Diebold and K. S. Hagen, *Inorg. Chem.*, 1998, **37**, 215–223.
27 A. Machkour, D. Mandon, M. Lachkar and R. Welter, *Inorg. Chim. Acta*, 2005, **358**, 839–843.
28 We even found that upon exposure to diethyl ether, this solvent coordinated our complexes and could only be removed by several prolonged washings of the complex in *N*-pentane under ultrasonic conditions.
29 Y. Zang, J. Kim, Y. Dong, E. C. Wilkinson, E. H. Appelman and L. Que, Jr., *J. Am. Chem. Soc.*, 1997, **119**, 4197–4205.
30 G. J. P. Britovsek, J. England and A. J. White, *Inorg. Chem.*, 2005, **44**, 8125–8134.
31 A. Company, L. Gomez, X. Fontrodona, X. Ribas and M. Costas, *Chem.–Eur. J.*, 2008, **14**, 5727–5731.
32 Y. Hitomi, S. Furukawa, M. Higushi, T. Shishido and T. Tanaka, *J. Mol. Catal. A: Chem.*, 2008, **288**, 83–86.
33 A. F. Trotman-Dickenson, *Adv. Free Radical Chem.*, 1965, **1**, 1–38.
34 G. V. Buxton, C. L. Greenstock, W. P. Helman and A. B. Ross, *J. Phys. Chem. Ref. Data*, 1988, **17**, 513–886.
35 S. Miyajima and O. Simamura, *Bull. Chem. Soc. Jpn.*, 1975, **48**, 526–530.
36 E. Finkelstein, G. M. Rosen and E. J. Rauckman, *J. Am. Chem. Soc.*, 1980, **102**, 4994–4999.
37 Y. Xia, A. L. Tsai, V. Berka and J. L. Zweier, *J. Biol. Chem.*, 1998, **273**, 25804–25808.
38 L. C. Wilms, J. C. S. Kleinjans, E. J. C. Moonen and J. J. Briede, *Toxicol. in Vitro*, 2008, **22**, 301–307.
39 M. Spulber and S. Schlick, *J. Phys. Chem. A*, 2010, **114**, 6217–6225.
40 B. Vileno, *PhD Thesis manuscript No. 3501*,2006, Ecole Polytechnique Fédérale de Lausanne, Switzerland.
41 L. Benhamou, M. Lachkar, D. Mandon and R. Welter, *Dalton Trans.*, 2008, 6996–7003.
42 J. England, C. R. Davies, M. Banaru, A. J. P. White and G. J. P. Britovsek, *Adv. Synth. Catal.*, 2008, **350**, 883–897.

43 M. P. Jensen, S. J. Lange, M. P. Mehn, E. L. Que and L. Que, Jr., *J. Am. Chem. Soc.*, 2003, **125**, 2113–2128.
44 D. H. R. Barton, A. H. Beck and D. K. Taylor, *Tetrahedron*, 1995, **51**, 5245–5254 Previous reactivity studies in acetonitrile with the same complex, $TPAFeCl_2(ClO_4)$, showed that tertbutyl hydroperoxide was efficient in promoting the stoichiometric formation of haloalkanes and some cyclohexanol/one when an excess of oxidant was used. See: T. Kojima, R. A. Leising, S. Yan and L. Que, Jr., *J. Am. Chem. Soc.*, 1993, **115**, 11328–11335.
45 C. Kim, K. Chen, J. Kim and L. Que, Jr., *J. Am. Chem. Soc.*, 1997, **119**, 5964–5965.
46 K. Chen and L. Que, Jr., *J. Am. Chem. Soc.*, 2001, **123**, 6327–6337.
47 The obvious consequence is to decrease the yield: in general, in biomimetic catalysis involving peroxides, the yield is calculated on the consumption of oxidant.
48 Y. Mekmouche, S. Ménage, C. Toia-Duboc, M. Fontecave, J.-B. Galey, C. Lebrun and J. Pecaut, *Angew. Chem., Int. Ed.*, 2001, **40**, 949–952.
49 This is one of the *a posteriori* justifications for the choice of $FeCl_2$ as the source of metal for all complexes already reported by our group.
50 D. H. Chin, J. Del Gaudio, G. La Mar and A. Balch, *J. Am. Chem. Soc.*, 1977, **99**, 5486–5488.
51 A. Wada, S. Ogo, S. Nagatomo, T. Kitagawa, Y. Watanabe, K. Jitsukawa and H. Masuda, *Inorg. Chem.*, 2002, **41**, 616–618.
52 D. H. R. Barton, *Tetrahedron*, 1998, **54**, 5805–5817.
53 See for instance: G. Strukul, Ed., *Catalytic Oxidations with Hydrogen Peroxide as Oxidant. Catal. Met. Complexes*, 1992, 9, Dordrecht, The Netherlands.
54 J. L. Roberts, Jr., M. M. Morrison and D. T. Sawyer, *J. Am. Chem. Soc.*, 1978, **100**, 329–330.
55 S. Venkataraman, *Journal of the Indian Chemical Society*, 1940, **17**, 297–303 Ref. 46 and 47: a 1 : 1 mixture of pyridine and acetic acid provides a poorly-defined compound termed pyridinium acetate, which in solution equilibrates with its conjugated base/acid.
56 J. Hurwic, J. Michalczyk and K. Pogorzelska, *Roczniki Chemii*, 1957, **31**, 265–275.
57 We prefer the term "radical process" to the "Fenton process", which is sometimes used, because historically, the Fenton reaction corresponds to the reaction of hydrogen peroxide, not molecular dioxygen, with metal salts.
58 The main reaction is the formation of the alcohol. The fact that some ketone is formed and particularly not by oxidation of the alcohol, suggests that some oxy form $[Fe(O_2)]$ might be protonated by acetic acid to generate radicals, converting cyclohexane into cyclohexanone.
59 G. B. Shul'pin and G. Süss-Fink, *J. Chem. Soc. Perkin Trans.*, 1995, 1459–1463.

